Photodetachment cross sections for $He^- {}^4P$

R. V. Hodges, M. J. Coggiola, and J. R. Peterson
Molecular Physics Laboratory, SRI International, Menlo Park, California 94025
(Received 17 June 1980)

Absolute photodetachment cross sections for $He^- {}^4P^o$ have been obtained at discrete photon energies between 0.12 and 4.0 eV by normalizing the He photodetachment products from a 1.3-keV He^- beam to those from autodetachment over a known path length, and making use of the known metastable lifetimes. The cross section reaches 1.2×10^{-16} cm^2 at 0.12 eV (40 meV above threshold), falls to 1×10^{-17} cm^2 at 4.0 eV, and exhibits several distinct features associated with excited He product states.

I. INTRODUCTION

The $1s2s2p\ {}^4P^o$ state of He^- is an unusual member of the class of core-excited atomic states that lie in the electronic continuum but are metastable against both autoejection of electrons and radiative decay. In 1955 Holøien and Midtdal[1] showed theoretically that $He^-\ {}^4P$ lies energetically below its parent $1s2s\ 2^3S$ state, and as it is metastable against autodetachment to the $^1S_0$ ground state, this result explained the experimental observation of He^- by Hiby in 1932.[2] Holøien and Geltman[3] later calculated the binding energy to be $\gtrsim$33 meV with respect to 2^3S. It was subsequently found to be 80 ± 2 meV by Brehm, Gusinow, and Hall[4] who measured the kinetic energies of photodetached electrons. Later the fine structure states of He^- were studied by Novick and co-workers, who measured their autodetachment lifetimes[5] and energy intervals.[6]

This ion offers an opportunity to study characteristics of doubly-excited atoms and to test theoretical calculations of energy levels and widths of higher autodetaching states. Numerous detailed calculations have been made of the He^- doublet resonances that appear in e-He scattering. However, comparatively little work has been done on the quartet states, many of which can likely be studied in very high resolution via photodetachment. Because of its low threshold energy for detachment, He^- also allows a study of the behavior of the photodetachment cross section over a wide range of photon wavelengths using available laser sources.

While determining the He^- electron binding energy, Brehm *et al.*[4] were also able to estimate (to within a factor of 2) the photodetachment cross section at 514.5 nm. However, until now no other photodetachment measurements have been reported.[7] We report here measurements of the photodetachment cross section of He^- at a number of discrete photon energies between 0.12 and 4.0 eV.[8]

II. EXPERIMENTAL METHOD

A 1300-eV beam of He^- was prepared from He^+ by two successive electron capture reactions in alkali vapor, as was first done by Donnally and Thoeming[9] using cesium, and later by Brehm *et al.*[4] and Novick *et al.*[5,6] using potassium. In this work, sodium was chosen as a target vapor because it has been shown[10] that the $He^+ + Na$ reaction yields 90% He 2^3S at our beam energies, whereas the other alkalies produce at least 30% 2^1S. The latter can yield only the doublet states of He^-, which rapidly autodetach.

We used an existing apparatus[11] which normally produces neutral rare-gas metastable atoms by single electron capture of the corresponding ion in an alkali vapor. The He^+ ion beam is formed by direct extraction from a dc discharge source. The beam is accelerated to its final kinetic energy and magnetically mass analyzed before being focused into a 6.7 cm long differentially pumped charge-exchange cell. Alkali vapor pressures of about 0.5 mtorr are used to produce neutral beams under single-collision conditions. However, in this experiment the Na vapor pressure was increased to ~10 mtorr where He^- production was about 0.1% of the incident He^+. In a separate vacuum chamber, the He^- component was electrostatically separated from He^0 and He^+ as shown in Fig. 1, and was intersected by a laser beam midway along a field-free drift region. Downstream, a second deflector removed residual ions leaving only neutral atoms formed from He^- in the drift region by photodetachment, autodetachment, or collisional detachment. These atoms entered the detector, where they struck a stainless steel surface at 45°, ejecting secondary electrons which were accelerated into a channeltron multiplier. Potentials on an entrance grid, the secondary emission surface, and the channeltron cone were adjusted to give optimum collection of the secondary electrons while rejecting electrons that originated outside the detector. The multi-

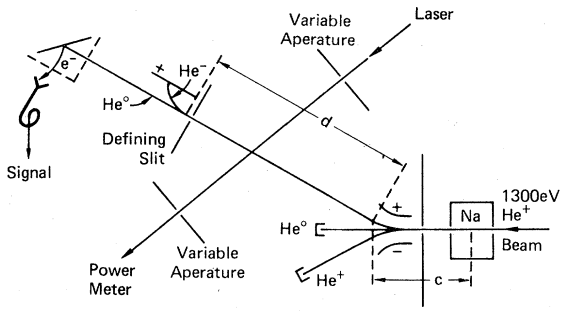

FIG. 1. Schematic diagram of the interaction region.

plier output was fed to appropriate pulse counting electronics. Several lasers were used as photon sources: a line-tunable cw CO_2 laser, cw Nd:YAG, argon and krypton ion lasers, and a pulsed rare-gas–halide excimer laser which was used alone and as a pump for a dye laser.

The photodetachment of a uniform ion beam of cross sectional area A, propagating along the x axis, and intersected by a laser beam propagating along the y axis, can be described by the equation

$$i_p/i_- = \sigma \int\int\int \frac{\Phi(x,z)}{A}\,dt\,dy\,dz, \quad i_p/i_- \ll 1 \qquad (1)$$

where σ is the photodetachment cross section, i_p is the equivalent current of photodetached He, i_- is the incident He^- current, and the integration extends over the time of interaction and the spatial overlap of the two beams in the y-z plane.

A major problem in obtaining reliable data was the evaluation of this integral. We found that consistent results could only be obtained by careful measurements of the laser-beam spatial distribution $\Phi(x,z)$, for each cross-section measurement. The laser beam was assumed to be cylindrically symmetric and thus $\Phi(x,z)$ could be expressed as $\Phi(r)$. This distribution was determined by measuring the laser power transmitted through each of two apertures of variable radius r at the entrance and exit windows of the interaction chamber. Measurements were made at six to eight values of r for each aperture by stopping down one aperture with the other fully open. The data were satisfactorily fitted to the Gaussian form

$$\Phi(r,\alpha) = P(\pi\alpha^2 h\nu)^{-1}\exp(-r^2/\alpha^2),$$

where P is the laser power, $h\nu$ is the photon energy, and α is the beam radius parameter. As the laser beam traversed the 1 m between apertures, α increased by 10–25%. The value of α at the laser-ion beam intersection was calculated assuming a linear change in α with distance. Values of α varied widely with laser power and wavelength, but the cross sections derived according to the procedure described below were internally consistent from day to day.

The height of the ion beam was defined by a 1.5-mm slit at the entrance to the final deflector. This slit was wide enough (8 mm) to accept the full width of the ~3-mm diameter ion beam parallel to the laser axis. For an ion beam of velocity v and height $2b$, Eq. (1) becomes

$$i_p/i_- = \sigma\int_{-b}^{b}\frac{1}{2b}\left[\int_{-\infty}^{\infty}\frac{P}{\pi\alpha^2 h\nu}\exp(-r^2/\alpha^2)\right]\frac{dx}{v}dz, \qquad (2)$$

$$= \frac{\sigma P}{vh\nu}\,\frac{1}{2b}\,\mathrm{erf}\left(\frac{b}{\alpha}\right). \qquad (3)$$

A noteworthy aspect of these experiments was the use of the metastability of He^- and the known lifetimes of the $J=\frac{1}{2}$, $\frac{3}{2}$, and $\frac{5}{2}$ substates to obtain absolute cross sections without determining the detector sensitivity. This was accomplished by normalizing the signal produced by photodetached neutrals to the steady background signal resulting from autodetachment ($\gtrsim 70\%$) and collisional detachment ($\lesssim 30\%$). The background signal i_b is described by

$$i_b/i_- = (R_a + k_c p)t$$
$$= (R_a + k_c p)d/v, \quad i_b/i_- \ll 1 \qquad (4a)$$

where R_a and $k_c p$ are the autodetachment and collisional detachment rates, p is the pressure, and d is the distance between the two deflectors that define the ion drift path (see Fig. 1). The collisional detachment rate constant k_c was determined relative to R_a from the slope m of a plot of background signal versus pressure.[12] The pressure was altered by throttling the gate valve on the interaction chamber diffusion pump. Thus,

$$i_b/i_- = R_a(1+mp)d/v. \qquad (4b)$$

The three He^- sublevels, $^4P_{5/2}$, $^4P_{3/2}$, and $^4P_{1/2}$, autodetach with lifetimes of 500 ± 200, 10 ± 2, and 16 ± 4 μsec, respectively.[5] Because the total fine structure splittings are less than 8 GHz (3×10^{-5} eV),[6] and the polarizabilities of all three states are expected to be equal, the population of the $\frac{5}{2}$, $\frac{3}{2}$, and $\frac{1}{2}$ He^- ^4P states formed from the electron capture of He 2^3S in sodium should be purely statistical. Novick and Weinflash[5] found this to be the case for He^- produced in potassium, and there is no intrinsic difference in production via the sodium reaction. The autodetachment rate, R_a, in the drift region d was thus calculated from the expression

$$R_a = \frac{f_{5/2}}{\tau_{5/2}} + \frac{f_{3/2}}{\tau_{3/2}} + \frac{f_{1/2}}{\tau_{1/2}}, \qquad (5)$$

where f_n is the fraction of the population in the nth sublevel and τ_n is the corresponding lifetime.

The population fractions are approximately constant during the beam's passage through the short drift region, but differ slightly from the original statistical distribution by small factors easily calculable from the lifetimes and the 1.7-μsec flight time from the point of formation to the drift region (region c in Fig. 1). The length of region c was estimated by assuming that the majority of the He^- ions were formed near the center of the charge-transfer oven. This assumption leads to a value of $c = 43.6$ cm. The uncertainty introduced by this assumption is much smaller than that due to the uncertainties in the lifetimes. The second field-free drift region (region d in Fig. 1) extends between the points within the two deflectors at which tangents to the ion trajectory are just able to enter the detector. This distance was calculated from the deflector geometry and the detector aperture radius to be 5.1 cm. Evaluation of Eq. (5) using these values gives $R_a = (4.1 \pm 0.7) \times 10^4$ sec^{-1}.

Equations (3) and (4) are readily combined to yield an expression for σ as follows:

$$\sigma = \frac{i_p}{i_b} \frac{R_a(1+mp)d2bh\nu}{P \sin(60)\,\mathrm{erf}(b/\alpha)} . \qquad (6)$$

The factor sin(60) corrects for the fact that our laser-ion beam intersection angle is 60° rather than 90°.

The ratio method used here assumed that all neutral He products are detected with equal efficiencies. While the autodetached neutrals are $^1S_0$, the photodetached products are detected as 2^3S. Since all product detection is via single particle counting, it is only necessary that these two species have secondary electron-ejection coefficients (γ) in excess of unity at 1300 eV for them to be detected with equal probability. Independent measurements[13] of the secondary ejection coefficients were made at 45° incidence for the ground state ($\gamma \approx 1.5$) and excited He atoms ($\gamma^* \approx 1.9$) verifying that this requirement was met.

The experiment was performed by chopping the photon beam and accumulating the counts from the neutral He detector corresponding to laser on and off in the two channels of a PAR model 1112 processor. The ratio i_p/i_b is given by the ratio of the difference count to the background count. This ratio varied between 10^{-4} and 10^{-2} depending on laser power and wavelength.

In the pulsed laser experiments at 308 and 380 nm, time-of-arrival spectra of neutral He following the laser pulse were obtained with a time-to-amplitude converter and a multichannel analyzer operated in the pulse-height analysis mode. Photodetached He atoms appeared as a peak superimposed on a continuous background of autodetached and collisionally detached He. The cross section was calculated by normalizing the area under the peak to the background using a formalism similar to that described for the cw case.

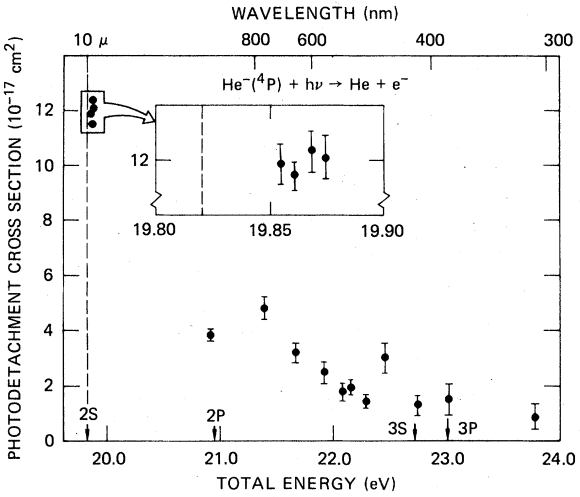

FIG. 2. Photodetachment cross section as a function of total energy relative to $He\,^1S_0$ (lower scale) and photon wavelength (upper scale). The arrows indicate outgoing excited He states.

III. RESULTS AND DISCUSSION

Results are presented in Fig. 2, and listed in Table I. The error bars shown are the relative uncertainties, which include the statistical counting uncertainty, and the relative uncertainties in α, P, and p. An absolute uncertainty of ±30% is assigned to the data on the basis of the uncertainties in the autodetachment rate (16%),[14] $k_c p$ (10%), d (10%), and the laser-ion beam overlap (15%).

The data in Fig. 2 are plotted against the total

TABLE I. Absolute $He^- 2\,^4P$ photodetachment cross sections.

λ(nm)	Laser	$\sigma(10^{-17}$ cm$^2)$
10741	$CO_2 - P(34)$	11.8
10275	$CO_2 - R(16)$	11.4
9657	$CO_2 - P(32)$	12.3
9282	$CO_2 - R(18)$	12.0
1060	Nd:YAG	3.9
752.5	Kr^+	4.7
647.1	Kr^+	3.3
568.2	Kr^+	2.5
530.9	Kr^+	1.8
514.5	Ar^+	2.0
488.0	Ar^+	1.3
457.9	Ar^+	3.0
413.1	Kr^+	1.3
380.0	XeCl + BBQ	1.5
308.0	XeCl	0.8

electronic energy relative to He $^1S_0$, $E = h\nu + 19.74$ eV, assuming that $He^- {}^4P$ lies 80 meV below He 2^3S, as measured by Brehm *et al.*,[4] although recent calculations argue for a slightly lower value.[15] The locations of the lowest He triplet states are indicated on the abscissa. The 2^3S photodetachment threshold is indicated by a vertical dashed line. At this threshold, the transition $1s2s2p + h\nu \rightarrow 1s2s\,2^3S + \epsilon s$ (or ϵd) yields predominantly s-wave electrons, and the cross section should behave[16,17] as $\nu(\nu - \nu_0)^{1/2}$, with an infinite slope at ν_0. The four CO_2 laser measurements near 10 μm are roughly equally spaced in energy between 35 and 53 meV above the threshold, as shown in the energy-magnified inset in Fig. 2. These points represent the largest cross sections observed. Considerably care was taken to reduce the uncertainties in these points. The lack of any strong energy dependence among them suggests that the maximum cross section is not much larger. It also indicates that the Wigner threshold law[16] does not extend this far above threshold because a $\nu(\nu - \nu_0)^{1/2}$ curve drawn from the 2^3S threshold through this region passes through the data in the expanded inset in Fig. 2 at about 70° to the horizontal and clearly does not fit the data. This result is not surprising; Hotop, Patterson, and Lineberger[18] found that the Wigner law is obeyed only within 5 meV of threshold for Se^- $^2P_{3/2} + h\nu \rightarrow Se\,^3P_2 + \epsilon s$.

Photodetachment cross sections (for a single outgoing state) generally peak at photon energies within a few times the threshold value and then fall off monotonically toward zero. If He^- behaves similarly, the cross section should peak at a total energy of $\lesssim$20 eV, and then fall off toward higher energies, at least to the 2^3P threshold at 20.96 eV. The photodetachment cross section at 20.91 eV, measured with a cw Nd:YAG laser (1.06 μm), lies below this threshold, and is thus expected to follow the smooth falloff from the peak value near 20 eV. However, the envelope established by extrapolating the points between 22.8 and 21.4 eV toward the 20.96-eV 2^3P threshold, indicates that a substantial increase in the cross section (by perhaps a factor of 2) occurs as the photon energy is increased through the 2^3P threshold. This increase would be more gradual than at the 2^3S threshold because here it involves an outgoing p wave ($1s2s2p\,^4P \rightarrow 1s2p\,^3P + \epsilon p$), and excluding interference effects the cross section should have a $\nu(\nu - \nu_0)^{3/2}$ threshold behavior.[17]

The point at 22.45 eV (from the 457.9-nm Ar^+ laser line) lies well above the envelope. We assume that this point is connected with a Feshbach resonance lying below the 3^3S state, possibly $1s3s3d\ ^4D^e$, which could rapidly autodetach and thus be fairly broad. Compton *et al.*[7] have also found a resonance in the vicinity of 470 nm. Oberoi and Nesbet[19] have calculated cross sections for electron scattering from He 2^3S and report a $^4D^e$ resonance at 22.56 eV with a width of 0.01 eV, which would correspond to a wavelength of 440 ± 1.5 nm.

The two highest energy points were measured using a pulsed XeCl excimer laser both directly at 308 nm, and to pump a dye (BBQ) at 380 nm. The latter wavelength corresponds approximately to the 3^3P threshold at 23.01 eV. The dye laser was used to search for resonance effects at a number of close-lying wavelengths between 377 and 382 nm. However, the dye laser output was unstable from pulse to pulse both in profile and position, and the resulting scatter in the data was too great to detect small structure. We have therefore averaged all these dye laser data to yield a single value at 380 nm. This point seems to lie above the envelope and could result from an increase above the 3^3P threshold, but the uncertainties are too large to attach much significance to it.

The only previously reported photodetachment cross section of He^- is the estimate of $\sigma = 6 \times 10^{-18}$ cm^2 ($\pm 2x$) at 514.5 nm by Brehm *et al.*,[4] who measured electrons ejected in the direction of the electric vector of the laser photons. The present value of $(2.0 \pm 0.6) \times 10^{-17}$ cm^2 is larger, but possibly within the combined uncertainties. Because their experiment was primarily aimed at the measurement of electron energies rather than cross sections, we do not consider the disagreement to be serious.

When only one outgoing channel exists, such as below the 2^3P threshold, it is straightforward using detailed balancing[17] to calculate the radiative attachment cross sections $\sigma_a(E_e)$, where E_e is the electron energy for $e + He\,2^3S \rightarrow He^-\,^4P + h\nu$. We find at 10 μm, σ_a (0.04 eV) $= 1.6 \times 10^{-22}$ cm^2, and below the 2^3P threshold, σ_a (1.09 eV) $= 1.2 \times 10^{-22}$ cm^2. The corresponding radiative attachment rates are 1.4×10^{-15} cm^3 sec^{-1} and 1.1×10^{-14} cm^3 sec^{-1}, respectively. Because we do not know the final state branching ratios at higher photon energies, further calculations would be speculative. The inability to distinguish between different product channels is the main shortcoming of this experimental method. Its advantage for cross section measurements is the simplicity of collecting all products regardless of the photon wavelength or of the final state of the He atom.

IV. CONCLUSIONS

These measurements are clearly incomplete, in that no details of resonance characteristics were

studied, but they do show the general aspects of the cross-section magnitude and its dependence on photon energy. These absolute photodetachment cross sections provide a useful test for various approximate methods of calculating oscillator strengths of bound-free transitions for weakly bound electrons. The 1.2 $Å^2$ peak cross section measured here is nearly three times larger than that for H^- ($EA = 0.75$ eV) but is close to that calculated[20] for Li^- ($EA = 0.62$ eV). Further experimental studies in the region between the threshold (~15.5 μm) and the first maximum (~5–8 μm) would be very useful. Other important areas for further research are in the 300–500-nm region, which should include much resonance structure associated with the He^- quartet states analogous to the doublet states recently calculated by Nesbet,[21] and the 0.8–2 μm region which should include the $^4P^e$ resonance structure as well as the 2^3P threshold behavior.

This work was supported by the Office of Naval Research. We have benefited from conversations with D. L. Huestis and K. T. Gillen.

---

[1]E. Holøien and J. Midtdal, Proc. Phys. Soc. London Sec. A 68, 815 (1955).
[2]J. W. Hiby, Ann. Phys. Leipzig 34, 473 (1939).
[3]E. Holøien and S. Geltman, Phys. Rev. 153, 81 (1967).
[4]B. Brehm, M. A. Gusinow, and J. L. Hall, Phys. Rev. Lett. 19, 737 (1967).
[5]R. Novick and D. Weinflash, in *Precision Measurement and Fundamental Constants (Proceedings of the International Conference at Gaithersburg, Md., 1970)*, edited by D. N. Langenberg and B. N. Taylor, National Bureau of Standards Special Publication No. 343 (U. S. GPO, Washington, D. C., 1971), pp. 403–410.
[6]D. L. Mader and R. Novick, Phys. Rev. Lett. 29, 199 (1972); 32, 185 (1974).
[7]Measurements are also being carried out currently at Oak Ridge National Laboratory by R. N. Compton and co-workers, J. Phys. B (unpublished).
[8]For a preliminary report, see: R. V. Hodges, M. J. Coggiola, J. R. Peterson, Abstracts of the 7th International Conference on Atomic Physics, Massachusetts Institute of Technology, Cambridge, 1980 (unpublished), p. 180.
[9]B. L. Donnally and G. Thoeming, Phys. Rev. 159, 87 (1967).
[10]C. Reynaud, J. Pommier, Vu Ngoc Tuan, and M. Barat, Phys. Rev. Lett. 43, 579 (1979).
[11]M. Hollstein, D. C. Lorents, J. R. Peterson, and J. R. Sheridan, Can. J. Chem. 47, 1858 (1969).
[12]Systematic measurements of the absolute collisional detachment cross section of He have recently been completed, M. J. Coggiola and R. V. Hodges (unpublished).
[13]R. V. Hodges, M. J. Coggiola, and K. T. Gillen (unpublished results).
[14]This uncertainty value was calculated assuming that the uncertainties in the three lifetimes were independent.
[15]A. V. Bunge and C. F. Bunge, Phys. Rev. A 19, 452 (1979) have calculated a binding energy of 77.4 meV with a reported accuracy of 0.2 meV. This value would shift all energies in Fig. 2 downward by 2.6 meV.
[16]E. P. Wigner, Phys. Rev. 73, 1002 (1948).
[17]H. Massey, *Negative Ions* (Cambridge University Press, London, 1976), p. 418.
[18]H. Hotop, T. A. Patterson, and W. C. Lineberger, Phys. Rev. A 8, 762 (1973).
[19]R. S. Oberoi and R. K. Nesbet, Phys. Rev. A 8, 2969 (1973).
[20]D. L. Moores and D. W. Norcross, Phys. Rev. A 10, 1646 (1974).
[21]R. K. Nesbet, J. Phys. B 11, L21 (1978).